JOC Article
pubs.acs.org/joc

Ferrocene-Substituted Nitrogen-Rich Ring Systems as Multichannel Molecular Chemosensors for Anions in Aqueous Environment

Fabiola Zapata, Antonio Caballero, Alberto Tárraga,* and Pedro Molina*

Departamento de Química Orgánica, Facultad de Química, Campus de Espinardo, Universidad de Murcia, E-30100 Murcia, Spain

pmolina@um.es; atarraga@um.es

Received November 2, 2009

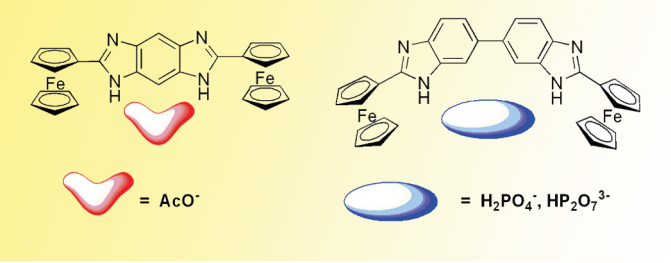

The synthesis, electrochemical, optical, and anion sensing properties of ferrocene-fused imidazole dyads are presented. Ferrocene-benzobisimidazole dyad **1** behaves as a highly selective redox, chromogenic and fluorescent chemosensor molecule for AcO^- anion in DMSO/H_2O: the oxidation redox peak is cathodically shifted ($\Delta E_{1/2} = -170$ mV), perturbation of the UV−vis spectrum, and the emission band is both red-shifted ($\Delta\lambda = 13$ nm) and increased (Chelation Enhanced Fluorescence, CHEF = 133) upon complexation with this anion. The related ferrocene-bisbenzimidazole dyad **2** has shown the ability for sensing both $H_2PO_4^-$ and $HP_2O_7^{3-}$ anions in the same medium. Upon complexation, it also displays a cathodic shift of the redox potential ($\Delta E_{1/2} = -90$ to 80 mV), as well as a clear perturbation of the UV−vis spectrum and an increase in the intensity of the emission band (CHEF = 97−37). However, such magnitudes are smaller than those exhibited by **1**. ^{1}H NMR studies have been carried out to obtain information about the molecular sites which are involved in the binding process.

Introduction

Anion recognition has attracted growing attention because they play a fundamental and important role in a wide range of chemical, biological, and environmental processes. Most chemosensors developed so far are chromogenic and/or fluorescent probes, which efficiently change their photophysical properties in the presence of anions.[1] On the other hand, ferrocene has also largely proved to be a simple and remarkably robust building block for the preparation of derivatives, which has been exploited in the electrochemical sensing of anions, both in organic and aqueous media. Electrochemical ferrocene-based receptors for anions are expected to show cathodic shifts in their redox-process when complexed to an anion, as they are easier to oxidize or harder to reduce than the free redox-active receptor.[2]

In this context, increasing efforts have been made to employ a variety of structural motifs to design efficient anion sensors. The nature of the interaction between anions and charge-neutral organic receptors is primarily based on hydrogen bonding. For this kind of receptors, the polarized N−H functional groups represent the most commonly seen anion interacting moiety in the literature.[3] In general, hydrogen bond-induced π-electron delocalization or basic anion-induced N−H deprotonation serves as the signaling output

*To whom correspondence should be addressed. Fax: (+34) 968 36 41 49.

(1) (a) Beer, P. D.; Gale, P. A. *Angew. Chem., Int. Ed.* **2001**, *40*, 486–516. (b) Martínez-Máñez, R.; Sancenón, F. *Chem. Rev.* **2003**, *103*, 4419–4476. (c) Amendola, V.; Esteban-Gomez, D.; Fabrizzi, L.; Lichelli, M. *Acc. Chem. Res.* **2006**, *39*, 343–353. (d) Gunnlaugsson, T.; Glynn, M.; Tocci, G. M.; Kruger, P. E.; Pfeffer, F. M. *Coord. Chem. Rev.* **2006**, *250*, 3094–3117. (e) Gale, P. A. *Acc. Chem. Res.* **2006**, *39*, 343–353.

(2) (a) Beer, P. D.; Cadman, J. *Coord. Chem. Rev.* **2000**, *205*, 131–155. (b) Beer, P. D.; Hayes, E. J. *Coord. Chem. Rev.* **2003**, *240*, 167–189. (c) Daniel, M.-C.; Astruc, D. *Chem. Rev.* **2004**, *104*, 293–346. (d) Beer, P. D.; Bayly, S. R. *Top. Curr. Chem.* **2005**, *255*, 125–16. (e) Molina, P; Tárraga, A.; Caballero, A. *Eur. J. Inorg. Chem.* **2008**, 3401–3417.

(3) Sessler J. L.; Gale, P.; Cho, W.-S. *Anion Receptor Chemistry*; RSC Publishing: Cambridge, UK, 2006.

Published on Web 12/07/2009 DOI: 10.1021/jo9023446

of the anion receptor interaction. Structural properties of benzimidazole molecules are important because they are largely governed by H-bonding. A large effect is observed due to the environment caused by the nonbonding electron pair on nitrogen, which plays an important role in the hydrogen bonding.[4]

In this sense, benzimidazole derivatives as anion-binding motif have attracted considerable attention very recently.[5] Some representative examples of the new familly of π-extended imidazole derivatives, the fluorescents benzobisimidazoles[6] and bisbenzimidazoles,[7] have been found to bind helix DNA and have proved to be suitable building blocks for the preparation of bimetallic complexes connected through a bis(carbene) linker.

Acetate is a critical component of numerous metabolic processes and production and oxidation rates of the acetate anion have been frequently used as an indicator of organic decomposition in marine sediments.[8] This anion is a posible tracer for malignancies and has been extensively investigated in prostate cancer and its metastases.[9]

For these reasons the rational design of efficient receptors for the Y-shaped acetate anion has attracted immense attention, and a number of chemosensor molecules for acetate have been reported in recent years.[10] Unfortunatly, these acetate chemosensors usually also display responses to other basic anions such as dihydrogenphosphate and fluoride, especially the latter.[11]

Pyrophosphate and related oxoanions play an important role in energy transduction in organism and control metabolic processes by participation in enzimatic reactions. ATP hydrolysis with the concomitant release of pyrophosphate is central to many biochemical reactions, such as DNA polymerization and the synthesis of cyclic adenosine monophosphate (c-AMP) catalyzed by DNA polymerase and adenylate cyclase, respectively.[12] Furthermore, the detection of released pyrophosphate has been examined as a real-time DNA sequencing method,[13] and it has also been considered important in cancer research.[14] Therefore, the detection and discrimination of these anions has been the main focus of the effort of several research groups. However, very few examples of effective selective fluorescent,[15] chromogenic,[16] or redox[17] chemosensors have so far been reported.

We wish to report now the preparation, redox, and electronic properties as well as the anion sensing properties of a family of ferrocene receptors, in which the metallocene unit is directly linked to a π-extended imidazole ring such as 2,2′-biferrocenyl benzobisimidazole **1** and 2,2′-biferrocenyl bisbenzoimidazole **2**. The benzobisimidazole architecture features two linearly opposed imidazole ring systems annulated to a common arene backbone while in the related bisbenzoimidazole skeleton the two fused heteroaromatic rings are linked through the 5 and 5′ positions. An important consequence of this arrangement is that the two ferrocene moieties are embodied within the system. The insertion of ferrocene subunits with redox characteristics within the ditopic fluorogenic heteroaromatic core may represent an important "added value" to this class of receptors. In fact, in this case, the ligand can be used not only to bind the substrates but also to signal their presence in solution, thanks to quantifiable changes of its redox and emission properties. Only the structurally related ditopic ligand 1,1′-bis(*N*-benzimidazole)ferrocene precursor of diiridium complexes

(4) (a) Chou, P. T.; Yu, W. S.; Chen, Y. C.; Wei, C. Y.; Martinez, S. S. *J. Am. Chem. Soc.* **1998**, *120*, 12927–12934. (b) Kumar, N.; Chakravorti, S.; Chowdhury, P. *J. Mol. Struct.* **2008**, *891*, 351–356. (c) Chowdhury, P.; Panja, S.; Chatterjee, A.; Battacharya, P.; Chakravorti, S. *J. Photochem. Photobiol., A* **2006**, *173*, 106–113.

(5) (a) Kang, J.; Kim, H. S.; Jang, D. O. *Tetrahedron Lett.* **2005**, *46*, 6079–6082. (b) Bai, Y.; Zhang, B.-G.; Xu, J.; Duan, C.-Y.; Dang, D.-B.; Liu, D.-J.; Meng, Q.-J. *New J. Chem.* **2005**, *29*, 777–779. (c) Moon, K. S.; Singh, N.; Lee, G. W.; Jang, D. O. *Tetrahedron* **2007**, *63*, 9106–9111. (d) Singh, N.; Jang, D. O. *Org. Lett.* **2007**, *9*, 1991–1994. (e) Yu, M.; Ln, H.; Zhao, G.; Lin, H. *J. Mol. Recognit.* **2007**, *20*, 69–73. (f) Kim, H. S.; Moon, K. S.; Jang, D. O. *Supramol. Chem.* **2006**, *18*, 97–1001. (g) Joo, T. Y.; Singh, N.; Lee, G. W.; Jang, D. O. *Tetrahedron Lett.* **2007**, *48*, 8846–8850. (h) Zapata, F.; Caballero, A.; Espinosa, A.; Tárraga, A.; Molina, P. *J. Org. Chem.* **2008**, *73*, 4033–4044. (i) Zapata, F.; Caballero, A.; Espinosa, A.; Tárraga, A.; Molina, P. *J. Org. Chem.* **2009**, *74*, 4787–4796. (j) Alfonso, M.; Sola, A.; Caballero, A.; Tárraga, A.; Molina, P. *Dalton Trans.* **2009**, 9653–9658.

(6) (a) Khramov, D. M.; Boydston, A. J.; Bielawski, C. W. *Org. Lett.* **2006**, *8*, 1831–1834. (b) Boydston, A. J.; Pecinovsky, C. S.; Chao, S. T.; Bielawski, C. W. *J. Am. Chem. Soc.* **2007**, *129*, 14500–14551. (c) Khramov, D. M.; Boyston, A.; Bielawski, C. W. *Angew. Chem., Int. Ed.* **2006**, *45*, 6186–6189.

(7) (a) Li, G. R.; Huang, J.; Zhang, M.; Zhou, Y. Y.; Zhang, D.; Wu, Z. G.; Wang, S. R.; Weng, X. C.; Zhou, X.; Yang, G. F. *Chem. Commun.* **2008**, 4564–4566. (b) Huang, J.; Li, G.; Wu, Z.; Song, Z.; Zhou, Y.; Shuai, L.; Weng, X.; Zhou, X.; Yang, G. *Chem. Commun.* **2009**, 902–904.

(8) (a) Shang, X.-F.; Xu, X.-F. *BioSystems* **2009**, *96*, 165–171. (b) Joo, T. Y.; Sing, N.; Lee, G. W.; Jang., D. O. *Tetrahedron Lett.* **2007**, *48*, 8846–8850.

(9) (a) Kuhajda, F. P.; Pizer, E. S.; Li, J. N.; Mani, N. S.; Frehywot, G. L.; Townsend, C. A. *Proc. Natl. Acad. Sci. U.S.A.* **2000**, *97*, 3450–3454. (b) Vavere, A. L.; Kridel, S. J.; Wheeler, F. B.; Lewis, J. S. *J. Nucl. Med.* **2008**, *49*, 327–334.

(10) (a) Fitzmaurice, R. J.; Kyne, G. M.; Douheret, D.; Kilburn, J. D. *J. Chem. Soc., Perkin Trans. 1* **2002**, 841–864. (b) Sessler, J. L; An, D.; Cho, W.-S.; Lynch, V. *J. Am. Chem. Soc.* **2003**, *125*, 13646–13647. (c) Wiskur, S. L.; Lavigne, J. L.; Metzger, A.; Tobey, S. L.; Lynch, V.; Anslyn, E. V. *Chem.—Eur. J.* **2004**, *10*, 3792–3804. (d) Descalzo, A. B.; Rurack, K.; Weisshoff, H.; Martínez-Mánez, R.; Marcos, M. D.; Amorós, P.; Hoffmann, K.; Soto, J. *J. Am. Chem. Soc.* **2005**, *127*, 184–200. (e) Sing, N. J.; Jun, E. J.; Chellappan, K.; Thangadurai, D.; Chandran, R. P.; Hwang, I.-C.; Yoon, J.; Kim, K. S. *Org. Lett.* **2007**, *9*, 485–488. (f) Kim, Y. K.; Lee, Y.-H.; Lee, H.-Y.; Kim, M. K.; Cha, G. S.; Ahn, K. H. *Org. Lett.* **2003**, *5*, 4003–4006. (g) Hu, S.; Guo, Y.; Xu, J.; Shao, S. *Org. Biomol. Chem.* **2008**, *6*, 2071–2075. (h) Gunnlaugsson, T.; Fruger, P. E.; Jensen, P.; Tierney, J.; Ali, H. D.; Hussey, G. M. *J. Org. Chem.* **2005**, *70*, 10875–10878. (i) Lin, Y.-C.; Chen, C.-T. *Org. Lett.* **2009**, *11*, 4858–4861.

(11) (a) Yu, X.; Lin, H.; Cai, Z.; Lin, H. *Tetrahedron Lett.* **2007**, *48*, 8615–8618. (b) Wang, T.; Bai, Y.; Ma, L.; Yan, X.-P. *Org. Biomol. Chem.* **2008**, *6*, 1751–1755. (c) Anzenbacher, P., Jr.; Palacios, M. A.; Jursikova, K.; Marquez, M. *Org. Lett.* **2005**, *7*, 5027–5030. (d) Kumar, S.; Luxami, V.; Kumar, A. *Org. Lett.* **2008**, *10*, 5549–5552.

(12) (a) Lipscombe, W. N.; Sträter, N. *Chem. Rev.* **1996**, *96*, 2375–2433. (b) Tabary, T.; Lu, L. *J. Immunol. Methods* **1992**, *156*, 55–60. (c) Nyrén, P. *Anal. Biochem.* **1987**, *167*, 235–238.

(13) Ronaghi, M.; Karamohamed, S.; Petterson, B.; Uhlen, M.; Nyren, P. *Anal. Biochem.* **1996**, *242*, 84–89.

(14) Xu, S.; He, M.; Yu, H.; Cai, X.; Tan, X.; Lu, B.; Shu, B. *Anal. Biochem.* **2001**, *299*, 188–193.

(15) (a) Fabbrizzi, L.; Marcotte, N.; Stomeo, F.; Taglietti, A. *Angew. Chem., Int. Ed.* **2002**, *41*, 3811–3814. (b) Gunnalaugsson, T.; Davis, A. P.; O'Brien, J. E.; Glynn, M. *Org. Lett.* **2002**, *4*, 2449–2452. (c) Lee, D. H.; Kim, S. Y.; Hong, J.-I. *Angew. Chem., Int. Ed.* **2004**, *43*, 4777–4780. (d) Kanekiyo, Y.; Naganawa, R.; Tao, H. *Chem. Commun.* **2004**, 1006–1007. (e) Cho, H. K.; Lee, D. H.; Hong, J.-I. *Chem. Commun.* **2005**, 1690–1692. (f) Jang, Y. J.; Jun, E. J.; Lee, Y. J.; Kim, Y. S.; Kim, J. S.; Yoon, J. *J. Org. Chem.* **2005**, *70*, 9603–9606. (g) McDonough, M. J.; Reynolds, A. J.; Lee, W. Y.G.; Jolliffe, K. A. *Chem. Commun.* **2006**, 2971–2973. (h) Bazzicalupi, C.; Biagini, S.; Bencini, A.; Faggi, E.; Giorgi, C.; Matera, I.; Valtancoli, B. *Chem. Commun.* **2006**, 4087–4089. (i) Lee, H. N.; Swamy, K. M. K.; Kim, S. K.; Kwon, J.-Y.; Kim, Y.; Kim, S.-J.; Yoon, Y. J.; Yoon, J. *Org. Lett.* **2007**, *9*, 242–246. (j) Lee, H. N.; Xu, Z.; Kim, S. K.; Swamy, K. M. K.; Kim, Y.; Kim, S.-J.; Yoon, J. *J. Am. Chem. Soc.* **2007**, *129*, 3828–3829. (k) Swamy, K. M. K.; Kwon, S. K.; Lee, H. N.; Shantha Kumar, S. M.; Kim, J. S.; Yoon, J. *Tetrahedron Lett.* **2007**, *48*, 8683–8686.

(16) (a) Lee, D. H.; Im, J. H.; Son, S. U.; Young, K.; Hong, J.-I. *J. Am. Chem. Soc.* **2003**, *125*, 7752–7753. (b) Aldakov, D.; Anzenbacher, P., Jr. *J. Am. Chem. Soc.* **2004**, *126*, 4752–4753. (c) Nishiyabu, R.; Anzenbacher, P., Jr. *J. Am. Chem. Soc.* **2005**, *127*, 8270–8271.

(17) Anzenbacher, P., Jr.; Palacios, M. A.; Kursikova, K.; Marquez, M. *Org. Lett.* **2005**, *7*, 5027–5030.

SCHEME 1. Synthesis of Ferrocenyl-Substituted Benzobisimidazole 1 and Bisbenzimidazole 2 Derivatives[a]

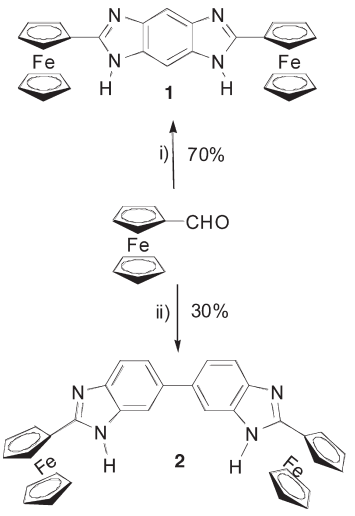

[a]Reagents and conditions: (i) 1,2,4,5-benzenetetramine tetrahydrochloride, Et_3N, nitrobenzene, 80 °C, 6 h; (ii) 3,3′-diaminobenzidine, nitrobenzene, 80 °C, 8 h.

which adopt Janus-like structures in the solid state have been described.[18]

Results and Discussion

Synthesis, Electrochemical, and Electronic Properties. Compound **1** was prepared in 70% yield from the reaction of 1,2,4,5-benzenetetramine tetrahydrochloride with ferrocenecarboxaldehyde in nitrobenzene at 80 °C in the presence of triethylamine. Likewise, compound **2** was prepared from 3,3′-diaminobenzidine and ferrocenecarboxaldehyde under very similar reaction conditions, albeit in lower yield (30%) (Scheme 1).

Reversibility and relative potentials of redox processes in the compounds were determined by cyclic (CV) and Osteryoung square wave (OSWV) voltammetry in 10^{-3} M DMSO solutions containing 0.1 M $[(n\text{-}Bu)_4N]PF_6$ as supporting electrolyte. The voltammograms of compounds **1** and **2**, containing two ferrocenyl groups bridged either by a benzene or biphenyl unit, show only a reversible two-electron oxidation peak at $E_{1/2} = 0.57$ and 0.53 V respectively versus decamethylferrocene (DMFc), indicating that the two metal centers in these compounds are electronically decoupled.[19]

The higher oxidation potential value observed for **1** is consistent with the greater electron-deficient character inherent to benzobisimidazole-based systems relative to benzimidazole analogues.[20]

The UV−vis data for **1** and **2** obtained in DMSO are consistent with most ferrocenyl chromophores in that they exhibit two charge transfer bands in the visible region.[21] These spectra contain two prominent absorption bands at $\lambda = 343$ nm ($\varepsilon = 30\,650\ M^{-1}\ cm^{-1}$) and at $\lambda = 361$ ($\varepsilon = 32\,490\ M^{-1}\ cm^{-1}$), for **1**, and at $\lambda = 332$ nm ($\varepsilon = 31\,080\ M^{-1}\ cm^{-1}$), for **2**, which can safely be ascribed to ligand-centered $\pi-\pi^*$ electronic transitions (L-π^*) (HE band). In addition, another weaker absorption is detected between 436 nm ($\varepsilon = 3669\ M^{-1}\ cm^{-1}$), for **1**, and 439 nm ($\varepsilon = 1730\ M^{-1}\ cm^{-1}$), for **2**, which is assigned to another localized excitation with a lower energy produced by two nearly degenerate transitions: either a Fe(II) d-d transition[22] or a metal−ligand charge-transfer (MLCT) process ($d_{\pi-\pi^*}$) (LE band). This assignment is in accordance with the latest theoretical treatment (model III) reported by Barlow et al.[23]

Receptors **1** and **2** exhibit very weak fluorescence in DMSO ($c = 10^{-5}$ M), with the excitation spectrum revealing $\lambda_{exc} = 380$ and 360 nm for **1** and **2**, respectively, as an ideal excitation wavelength. The emission spectra show one broad and structureless band at 428 and 405 nm, respectively, due to the heteroaromatic core, with rather low quantum yield ($\Phi = 3.8 \times 10^{-3}$ for **1** and 8.4×10^{-3} for **2**).

Sensing Properties. The binding and recognition ability of receptors **1** and **2** toward various anions (F^-, Cl^-, Br^-, AcO^-, NO_3^-, HSO_4^-, $H_2PO_4^-$, $HP_2O_7^{3-}$, $(COO)^{2-}$, $CH_2(COO)^{2-}$, and $C_6H_5{-}COO^-$) in the form of their corresponding tetrabutylammonium salts (TBA^+) have been investigated by cyclic (CV) and Osteryoung square-wave voltammetry (OSWV), spectroscopic measurements, and ^1H NMR spectroscopy. In general, the results show that ions F^-, Cl^-, Br^-, HSO_4^-, $(COO)^{2-}$, $CH_2(COO)^{2-}$, and $C_6H_5{-}COO^-$ do not cause significant changes in either redox potencial, absorption, or the fluorescence emission spectrum, whereas redox shift, red-shifted absorptions, and increased emission bands are observed upon the addition of AcO^-, NO_3^-, $H_2PO_4^-$, and $HP_2O_7^{3-}$ anions.

At first, the electrochemical properties of receptor **1** in the presence of variable concentrations of the above-mentioned set of anions were investigated by CV and OSWV voltammetry.[24] Titration studies with addition of those anions in H_2O ($c = 2.5 \times 10^{-2}$ M) to an electrochemical solution of the receptor **1** in DMSO ($c = 1 \times 10^{-3}$ M) demonstrate that while addition of AcO^- and NO_3^- anions promotes remarkable responses, addition of F^-, Cl^-, Br^-, HSO_4^-, $H_2PO_4^-$, $HP_2O_7^{3-}$, $(COO)^{2-}$, $CH_2(COO)^{2-}$, and $C_6H_5{-}COO^-$ anionic species had no effect on the CV or OSWV of this receptor, even when present in a large excess. Nevertheles, the results obtained on the stepwise addition of substoichiometric amounts of AcO^- and NO_3^- anions revealed two different electrochemical behaviors. For the AcO^- anion a typical "two wave behavior", with the appearance of a second wave at more negative potentials ($\Delta E_{1/2} = -170$ mV) together with corresponding to the free receptor, which is due to the anion complexed species, is clearly observed (Figure 1a), while for the NO_3^- anion a "shifting behavior" in which a

(18) Varnado, C. D., Jr.; Lynnch, V. M.; Bielawski, C. W. *Dalton Trans.* **2009**, 7253–7261.
(19) Zanello, P. *Inorganic Electrochemistry Theory: Practice and Application*; RSC: Cambridge, UK, 2003.
(20) Er, J. A. V.; Tension, A. G.; Kamplain, J. W.; Lynnch, V. M.; Bielawski, C. W. *Eur. J. Inorg. Chem.* **2009**, 1729–1738.
(21) Farrel, T.; Meyer-Friedrichsen, T.; Malessa, M.; Haase, D.; Saak, W.; Asselberghs, I.; Wostyn, K.; Caliz, K.; Persoons, A.; Heck, J.; Manning, A. R. *J. Chem. Soc., Dalton Trans.* **2001**, 2936 and references cited therein.
(22) Sohn, Y. S.; Hendrickson, D. N.; Gray, H. B. *J. Am. Chem. Soc.* **1971**, *93*, 3603–3612.
(23) Barlow, S.; Bunting, H. E.; Ringham, C.; Green, J. C.; Bublitz, G. U.; Boxer, S. G.; Perry, J. W.; Marder, S. R. *J. Am. Chem. Soc.* **1999**, *121*, 3715–3723.
(24) The OSWV technique has been employed to obtain well-resolved potential information, while the individual redox processes are poorly resolved in the CV experiments in which individual $E_{1/2}$ potential cannot be easily or accurately extracted from the data. Serr, B. R.; Andersen, K. A.; Elliot, C. M.; Anderson, O. P. *Inorg. Chem.* **1988**, *27*, 4499–4504.

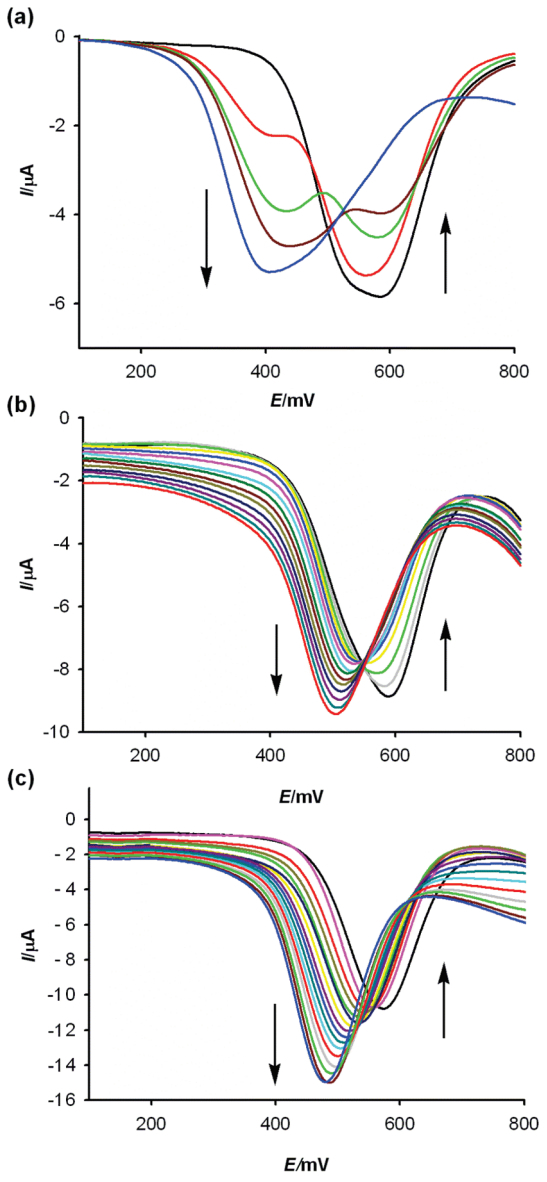

FIGURE 1. Evolution of the OSWV of the new receptors (1 mM in DMSO), when increasing amounts of the appropriate anion (c = 2.5×10^{-2} M in H_2O) were added, with $[(n\text{-}Bu)_4N]ClO_4$ as supporting electrolyte: (a) receptor **1** + AcO^-; (b) receptor **1** + NO_3^-; and (c) receptor **2** + $HP_2O_7^{3-}$.

second redox wave is negatively shifted ($\Delta E_{1/2}$ = −90 mV) compared to the free receptor appears (Figure 1b).[25]

Likewise, for receptor **2** under the same electrochemical conditions the ferrocene/ferrocenium redox peak showed a "shifting behavior" and a new oxidation peak emerged at a potential cathodically shifted from that of the free receptor in the presence of the oxoanions $HP_2O_7^{3-}$ ($\Delta E_{1/2}$ = −90 mV) and $H_2PO_4^-$ ($\Delta E_{1/2}$ = −80 mV) (Figure 1c).

Concerning the deprotonation/coordination dualism, the electrochemical data strongly support that the AcO^- anion induces formation of a hydrogen-bonded complex between receptor **1** and AcO^- anion, as well as receptor **2** does in the presence of $HP_2O_7^{3-}$ anion. Titrations with the strong base n-Bu_4NOH, which definitely leads to deprotonation, induced a remarkable cathodic shift of the oxidation peak of both the receptor **1** ($\Delta E_{1/2}$ = −380 mV) and receptor **2** ($\Delta E_{1/2}$ = −270 mV). A way to reveal the formation of hydrogen-bonded complexes under conditions of electrochemical titration is to suppress deprotonation by adding a small amount of acetic acid.[26] In preliminary experiments, we found that addition of up to 20 equiv of acetic acid did not affect neither CV or OSWV of receptors **1** and **2** in DMSO. Addition of AcO^- anion to an electrochemical solution of receptor **1** in DMSO in the presence of 20 equiv of acetic acid induced a cathodic shift of the oxidation peak ($\Delta E_{1/2}$ = −170 mV) similar to that observed in the absence of acid. Likewise, the addition of $HP_2O_7^{3-}$ anion to an electrochemical solution of receptor **2** in DMSO in the presence of 20 equiv of acetic acid induces the same change in the oxidation peak as that observed when 1 equiv of $HP_2O_7^{3-}$ anion was added ($\Delta E_{1/2}$ = −90 mV).

The anion binding ability of receptors **1** and **2** has also been examinied by UV−vis spectroscopy. Titration experiments for DMSO solutions of these ligands ($c = 1 \times 10^{-4}$ M) and the corresponding anions in H_2O ($c = 2.5 \times 10^{-2}$ M) were performed and analyzed quantitatively.[27] It is worth mentioning that no changes were observed in the UV−vis spectrum of receptor **1** upon addition of F^-, Cl^-, Br^-, NO_3^-, HSO_4^-, $H_2PO_4^-$, $HP_2O_7^{3-}$, $(COO)^{2-}$, $CH_2(COO)^{2-}$, and C_6H_5−COO^- anions, even in a large excess. However, significant modifications were observed upon addition of AcO^- anions.

Thus, the addition of increasing amounts of AcO^- ions to a solution of **1** caused the progressive appearance of a new band located at λ = 403 nm ($\varepsilon = 5580\ M^{-1}\ cm^{-1}$) as well as a decrease of the initial HE bands intensity. A well-defined isosbestic point at 373 nm indicates that a neat interconversion between the uncomplexed and complexed species occurs (Figure 2). Binding assays using the method of continuous variations (Job's plot) suggest a 1:1 binding model with a $K_a = 2.58 \times 10^3\ M^{-1}$.

In comparison to the above-mentioned results obtained with receptor **1**, the titration studies of receptor **2** toward the same set of anions and under the same conditions revealed a different behavior than **1** upon addition of AcO^-, $HP_2O_7^{3-}$, and $H_2PO_4^-$ anions (Figure 3). In this case, whereas $HP_2O_7^{3-}$ and $H_2PO_4^-$ anions promote a clear complexation process, the AcO^- anion does not induce any detectable change. It is worth mentioning that addition of $HP_2O_7^{3-}$ and $H_2PO_4^-$ anions elicited different optical responses. The most prominent feature observed upon addition of successive substoichiometric amounts of aqueous $HP_2O_7^{3-}$ is a progressive red shift of the HE band ($\Delta\lambda$ = 10 nm), whereas a progressive appearance of a new band located at λ = 384 nm ($\varepsilon = 9230\ M^{-1}\ cm^{-1}$) as well as a decrease of the initial HE band intensity upon addition of $H_2PO_4^-$ was also observed.

(25) Miller, S. R.; Gustowski, D. A.; Chen, Z. H.; Gokel, G. W.; Echegoyen, L.; Kaifer, A. E. *Anal. Chem.* **1988**, *60*, 2021–2024.

(26) Zapata, F.; Caballero, A.; Espinosa, A.; Tárraga, A.; Molina, P. *J. Org. Chem.* **2008**, *73*, 4034–4044.

(27) Specfit/32 Global Analysis System, 1999−2004, Spectrum Software Associates (SpecSoft@compuserve.com). The Specfit program was acquired from Biologic, S.A. (www.bio-logic.info) in January 2005. The equation to be adjusted by nonlinear regression using the above-mentioned software was $\Delta A/b = \{K_{11}\Delta\varepsilon_{HG}[H]_{tot}[G]\}/\{1 + K_{11}[H]\}$, where H = host, G = guest, HG = complex, ΔA = variation in the absorption, b = cell width, K_{11} = association constant for a 1:1 model, and $\Delta\varepsilon_{HG}$ = variation of molar absorptivity.

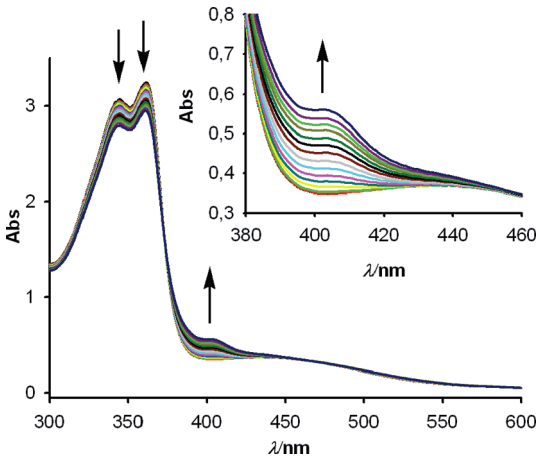

FIGURE 2. Evolution of the absorption spectra of receptor **1** ($c = 1 \times 10^{-4}$ M in DMSO) upon addition of increasing amounts of AcO^- anions ($c = 2.5 \times 10^{-2}$ M in H_2O). Arrows indicate the absorptions that increase or decrease during the experiment. An enlargement of the increase observed in the band at $\lambda = 403$ nm is shown in the inset.

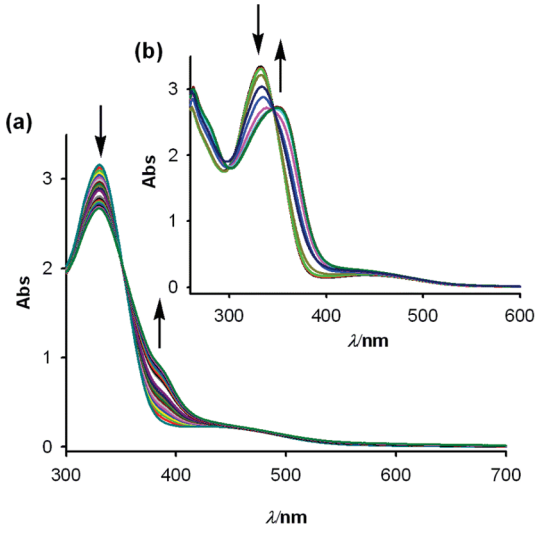

FIGURE 3. Changes in the absorption spectra of receptor **2** ($c = 1 \times 10^{-4}$ M in DMSO) upon addition of increasing amounts of (a) $H_2PO_4^-$ ($c = 2.5 \times 10^{-2}$ M in H_2O) and (b) $HP_2O_7^{3-}$ ($c = 2.5 \times 10^{-2}$ M in H_2O). Arrows indicate the absorptions that increase or decrease during the titration.

Well-defined isosbestic points at $\lambda = 300$ and 346 nm for $HP_2O_7^{3-}$ and at λ 384 nm for $H_2PO_4^-$, indicative of the presence of only two absorbing species in the solution, were found. In these cases, 1:1 binding models were also observed and the corresponding binding constants were also determined by the analysis of the spectral titration data by using the already mentioned software, $K_a = 3.28 \times 10^3$ M^{-1} for $HP_2O_7^{3-}$ and 6.30×10^3 M^{-1} for $H_2PO_4^-$.

From these data it may be concluded that perturbations of the UV−vis spectrum of receptor **1** upon addition of the trigonal AcO^- anion were similar to those observed in the spectrum of receptor **2** in the presence of the tetrahedral $H_2PO_4^-$ anion, which suggests similar binding modes. Moreover, the different responses observed in the spectrum of receptor **2** toward $HP_2O_7^{3-}$ anion are clearly indicative that

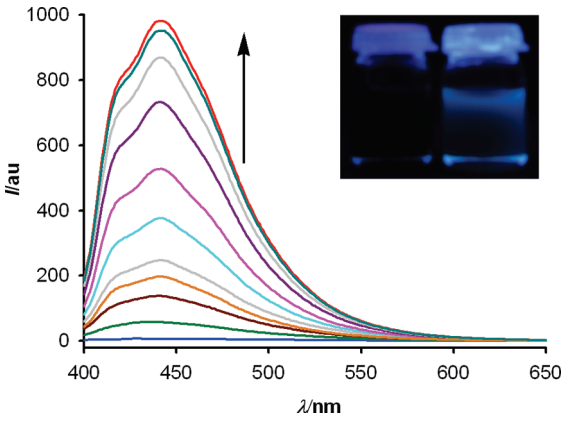

FIGURE 4. Changes in the fluorescence spectra of receptor **1** (deep blue line) ($c = 1 \times 10^{-5}$ M in DMSO) upon addition of increasing amounts of AcO^- ($c = 2.5 \times 10^{-3}$ M in H_2O) (red line). Inset: Visual changes in the fluorescence of receptor **1** (left) upon addition of AcO^- (right).

a different conformational disposition is adopted by the receptor for the complex formation.

Assessment of the anion affinities also came from observing the extent to which the fluorescence intensity of **1** and **2** was affected in the presence of anions. Receptor **1** in DMSO did not undergo any considerable change in its emission spectra; upon addition of F^-, Cl^-, Br^-, HSO_4^-, $H_2PO_4^-$, $HP_2O_7^{3-}$, $(COO)^{2-}$, $CH_2(COO)^{2-}$, and $C_6H_5{-}COO^-$ anions, it showed, however, a large CHEF (chelation-enhanced fluorescence)[28] effect when aqueous AcO^- anion was added and a relatively small CHEF effect upon addition of NO_3^-.

Thus, addition of 1 equiv of aqueous AcO^- to a solution of the receptor **1** in DMSO ($c = 1 \times 10^{-5}$ M) induced a red shift of the emission band from 428 to 441 nm ($\Delta\lambda = 13$ nm) accompanied by a remarkable increase of the intensity of the emission band (CHEF = 133), and the quantum yield ($\Phi = 0.27$) resulted in a 71-fold increase (Figure 4). In the presence of 1 equiv of NO_3^- anion, only an increase of the intensity of the emission band (CHEF = 37) and the quantum yield ($\Phi = 0.031$) was observed. From the fluorescence titration data, a 1:1 binding mode is deduced and the association constant was calculated to be 3.2×10^4 M^{-1} for AcO^-. The detection limit, calculated as three times the standard deviation of the background noise, was found to be 1.3×10^{-5} M (see the Supporting Information).

After addition of 1 equiv of aqueous $H_2PO_4^-$ anion to a solution of the receptor **2** in DMSO, the emission band was red-shifted by 25 nm, from 405 nm to 430 mn, increased by a CHEF = 97, and the fluorescence quantum yield increased by a factor of 46 ($\Phi = 0.39$). Similar but smaller changes were observed in the presence of aqueous $HP_2O_7^{3-}$, a 4-fold increased quantum yield ($\Phi = 0.033$) and a CHEF = 37 (Figure 5). The stoichiometry of the complexes was also determined by the changes in the fluorogenic response of **2** in the presence of varying concentrations of $H_2PO_4^-$ and $HP_2O_7^{3-}$ anions, the results indicating the formation of 1:1 complexes with association constants $K_a = 5 \times 10^4$ M^{-1} for $H_2PO_4^-$ and 5.7×10^4 M^{-1} for $HP_2O_7^{3-}$ and detection limits

(28) CHEF is defined as I_{max}/I_0, where I_{max} corresponds to the maximum emission intensity of the receptor−metal complex, while I_0 is the maximum emission intensity of the free receptor.

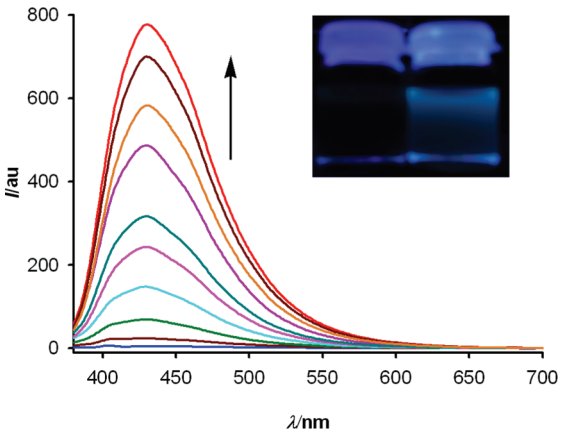

FIGURE 5. Changes in the fluorescence spectra of receptor **2** (deep blue line) ($c = 1 \times 10^{-5}$ M in DMSO) upon addition of increasing amounts of $H_2PO_4^-$ ($c = 2.5 \times 10^{-3}$ M in H_2O) (red line). Inset: Visual changes in the fluorescence of receptor **2** (left) upon addition of $H_2PO_4^-$ (right).

1.25×10^{-5} and 1.21×10^{-5} M, respectively (see the Supporting Information). No changes in the emission spectrum of receptor **2** were observed in the presence of the remaining tested anions.

These findings underscore the unprecedented multichannel selectivity of receptor **1** for AcO^- anions and receptor **2** for $H_2PO_4^-$, $HP_2O_7^{3-}$ anions in a relatively polar solvent (DMSO) where hydrogen bonding interactions between the N−H functional groups and the anions are usually weakened by competing solvent molecules.

The binding modes proposed from absorption and fluorescent data were further confirmed by electrospray mass spectrometry in the presence of the anions. The ESI-MS spectrum of receptor **1** in the presence of AcO^- anions shows a peak at m/z 585 corresponding to the 1:1 complex. The relative abundance of the isotopic cluster was in good agreement with the simulated spectrum of the [**1**·AcO^-] complex. Likewise, receptor **2** in the presence of the appropriate anion also showed peaks at m/z 699 and at 1019 attributable to the [**2**·$H_2PO_4^-$] and [**2**·HP_2O_7·(n-Bu_4N)]$^{2-}$ fragments, respectively (Figure 6).

To gain insight into the structures of complex formation of these receptors, we carried out ^{1}H NMR titration experiments. Figure 7 shows the ^{1}H NMR spectra of **1** in DMSO-d_6 solution before and after addition of different amounts of AcO^- anions ($c = 2.5 \times 10^{-2}$ M). The free receptor shows the characteristic signals corresponding to the protons within the mono- and unsubstituted Cp rings present in the two equivalent ferrocene moieties: two pseudotriplets at δ 4.45 and 5.02 ppm for the H_α and H_β, respectively, and a singlet at δ 4.09 ppm. Additionally, it presents another singlet at δ 7.50 ppm corresponding to the phenyl ring protons and a broad singlet, centered at δ 12.12 ppm, due to the NH present in the heterocyclic ring. However, a few important features were observed from the ^{1}H NMR spectra upon addition of increasing amounts of AcO^- anions: (i) some variations in chemical shifts are experienced by protons on the phenyl group, that is, the singlet is split into two new singlets one of which is high-field shifted upon complexation with the anion; (2) the signal intensity of the NH protons almost disappeared in the presence of 0.6 equiv of AcO^-; and (3) the

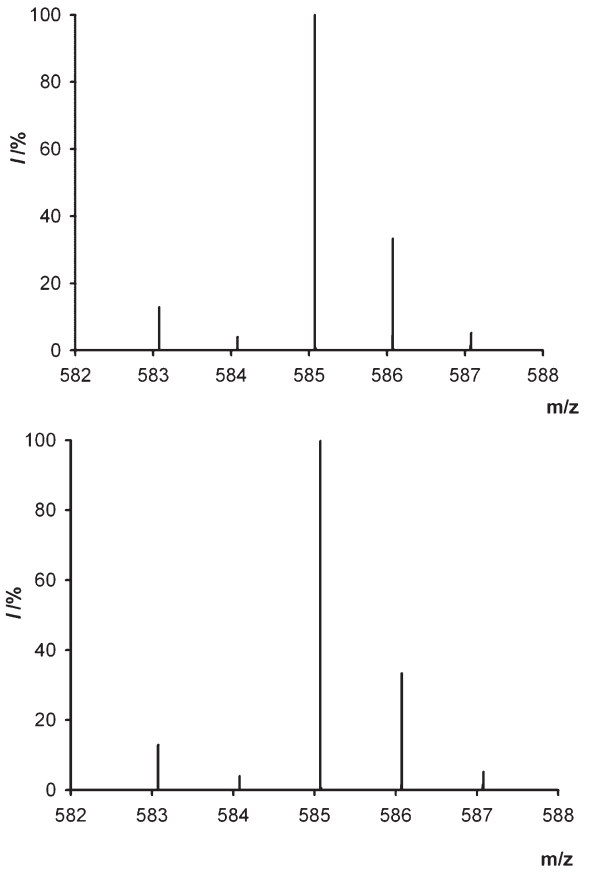

FIGURE 6. Experimental relative abundance of the isotopic cluster for [**1**·AcO^-] (top) and simulated (bottom).

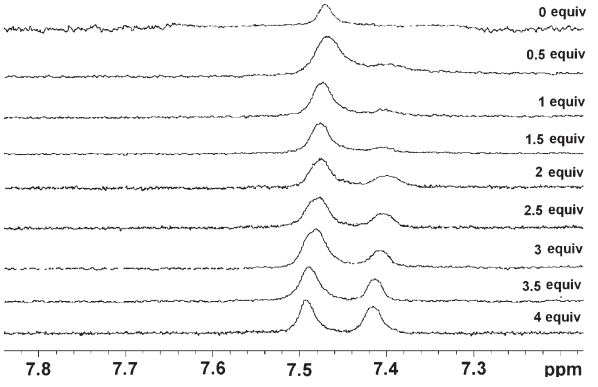

FIGURE 7. Evolution of the ^{1}H NMR spectra (aromatic region) of **1** in DMSO-d_6 upon addition of increasing amounts of AcO^- ($c = 2.5 \times 10^{-2}$ M in D_2O), from 0 to 4 equiv.

signals of the ferrocene unit in the free ligand were almost unaffected even in the presence of 4 equiv of AcO^- although at this moment, a very slight splitting of the signals was observed.

Anion-induced chemical shift changes in the ^{1}H NMR spectra of the related receptor **2**, providing additional evidence for its interaction with the anions, were also studied. It is worth mentioning that while the NH and ferrocenyl protons appear as clearly defined signals in the ^{1}H NMR spectrum, those corresponding to the phenyl ring protons are

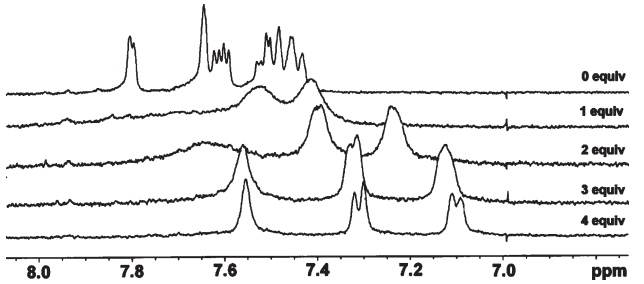

FIGURE 8. Evolution of the ^{1}H NMR spectra (aromatic region) of **2** in DMSO-d_6 upon addition of increasing amounts of $HP_2O_7^{3-}$ ($c = 2.5 \times 10^{-2}$ M in D_2O), from 0 to 4 equiv.

significantly complex due to the different tautomers in which **2** can exist and to the free rotation about its $C_{Ar}-C_{Ar'}$ bond, which could lead to the formation of different atropoisomers. Direct evidence to support this assumption came from the ^{1}H NMR spectrum obtained at 50 °C, which shows the expected pattern for such protons: two broad singlets at δ 7.45 and 7.62 ppm and one singlet at δ 7.77 ppm.

^{1}H NMR titrations of **2** with the above-mentioned set of anions clearly evidenced that only the addition of $HP_2O_7^{3-}$ and $H_2PO_4^-$ anions promoted significant perturbations on the proton signals of this receptor, although the type of perturbations produced are dependent on the anion added. Thus, upon addition of increasing amounts of a solution of $HP_2O_7^{3-}$ ($c = 2.5 \times 10^{-2}$ M in D_2O) to a DMSO-d_6 solution of **2** the signals corresponding to the ferrocenyl protons were upfield shifted by $\Delta\delta = -0.08$ (H_α), $\Delta\delta = -0.27$ (H_β), and $\Delta\delta = -0.12$ (unsubstituted Cp ring). Furthermore, the multiplet corresponding to the phenyl ring protons was split into one singlet and two doublets suggesting that the complexation of this anion should prevent to some extent both the tautomeric and atropoisomeric effects observed in the free ligand. Simultaneously, the signal corresponding to the NH protons progressively moved downfield and decreased in intensity until 1 equiv was added, at which point it almost disappeared (Figure 8).

By contrast, when $H_2PO_4^-$ anion was added the ferrocenyl H_α and H_β protons were modestly shifted by $\Delta\delta = -0.04$ (H_α) and +0.07 ppm (H_β), while the chemical shift corresponding to the protons within the unsubstituted Cp ring remained almost unaltered. Moreover, the multiplet of the phenyl ring protons around $\delta = 7.43-7.79$ ppm was slightly split into one multiplet ($\delta = 7.4-7.6$ ppm) corresponding to the H6 and H7 protons within the aromatic ring and a broad singlet ($\delta = 8.4$ ppm) due to the H4 proton whose intensity progressively increased until 4 equiv of anion were added. The NH signal was also downfield shifted with a progressive decrease of its intensity until complete disappearance when 1 equiv of anion was added (Figure 9).

These features clearly suggest that in both cases the imidazole NH groups were involved in the complexation of both tetrahedral anions. However, the different changes observed in the ^{1}H NMR spectra during the titration with both anions seem to demonstrate that different conformations of the free ligand should be implied in the complex formation. From the spectroscopic date (UV−vis and ^{1}H NMR) it seems plausible that a planar or almost planar conformation of receptor **2** is present in the complex formation with the $H_2PO_4^-$ anion, whereas a twisted conformation

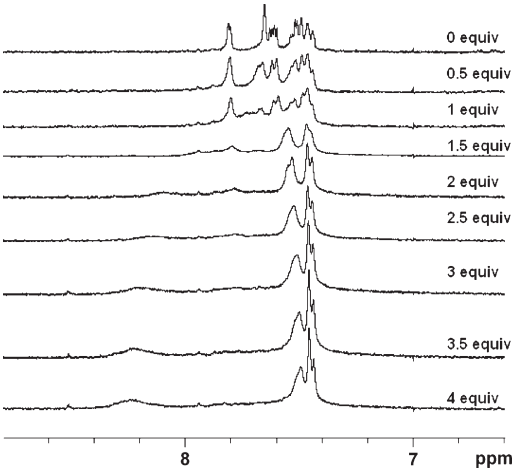

FIGURE 9. Evolution of the ^{1}H NMR spectra (aromatic region) of **2** in DMSO-d_6 upon addition of increasing amounts of $H_2PO_4^-$ ($c = 2.5 \times 10^{-2}$ M in D_2O), from 0 to 4 equiv.

CHART 1. Plausible Courses for the Formation of the Complexes

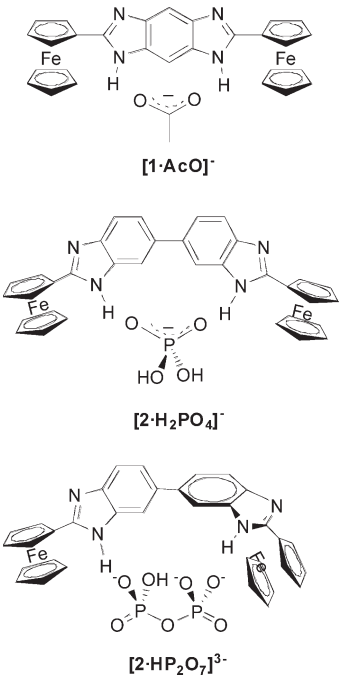

should participate in the formation of the [**2** $HP_2O_7]^{3-}$ complex (Chart 1).

Conclusion

The new ferrocene benzobisimidazole-based system **1** prepared has a highly flat rigid structure with a large π system, and exhibits high binding affinity and sensitivity for the Y-shaped acetate anions in DMSO/H_2O: a remarkable cathodic shift of the redox peak of the Fe(II)/Fe(III) couple along with a red-shift of the emission band and an increase of the emission intensity.

The related receptor **2** in DMSO senses aqueous $H_2PO_4^-$ and $HP_2O_7^{3-}$ anions through different channels: a red-shift of the emission band with an important chelation enhanced fluorescence effect and a large cathodic shift of the ferrocene

oxidation peak. The recognition event has also been studied by ^{1}H NMR spectroscopy. The magnitudes of these perturbations are smaller for receptor **2** than those exhibited by **1**.

Experimental Section

Preparation of 2,2′-Diferrocenyl-1*H*-benzo[1,2-*d*,4,5-*d*′]bisimidazole 1. To a solution of 1,2,4,5-benzenetetramine tetrahydrochloride (0.24 g, 2.37 mmol) in nitrobenzene (5 mL) were added triethylamine (0.426 g, 4.22 mol) and ferrocenecarboxaldehyde (0.25 g, 1.16 mmol). The reaction mixture was heated at 80 °C for 6 h and the resulting solid was filtered, washed with H_2O (2 × 25 mL), and crystallized from diethyl ether to give **1** as a crystalline solid in 70% yield. Mp >300 °C. ^{1}H NMR (DMSO-d_6) δ 4.09 (s, 10H), 4.45 (st, 4H), 5.02 (st, 4H), 7.50 (s, 2H), 12.1 (br s, 2H). The ^{13}C NMR was impossible to obtain due to the low solubility of this compound in the commonly used deuterated solvents. MS (FAB$^+$) m/z (rel intensity) 527 ($M^+ + 1$, 100). Anal. Calcd for $C_{28}H_{22}Fe_2N_4$: C, 63.91; H, 4.21; N, 10.65. Found: C, 64.10; H, 4.35; N, 10.45.

Preparation of 2,2′-Diferrocenyl-5,5′-bis(benzimidazole) 2. To a solution of 3,3′-diaminobenzidine (0.52 g, 2.37 mmol) in nitrobenzene (5 mL) was added ferrocenecarboxaldehyde (0.25 g, 1.16 mmol). The reaction mixture was heated at 80 °C for 8 h. The precipitated solid was filtered, washed with diethyl ether (2 × 25 mL), chromotagraphed on a silica gel column with CH_2Cl_2/MeOH (9:1) as eluent, and, finally, crystallized from acetonitrile to give **2** in 30% yield. Mp >300 °C. ^{1}H NMR (DMSO-d_6, 25 °C) δ 4.12 (s, 10H), 4.51 (st, 4H), 5.06 (st, 4H), 7.43−7.52 (m, 3H), 7.60−7.64 (m, 2H), 7.80−7.81 (m, 1H), 12.4 (m, 2H). ^{1}H NMR (DMSO-d_6, 50 °C) δ 4.10 (s, 10H), 4.45 (st, 4H), 5.03 (st, 4H), 7.45 (br s, 2H), 7.62 (br s, 2H), 7.77 (s, 2H), 12.11 (br s, 2H). ^{13}C NMR (DMSO-d_6, 25 °C) 68.9 (CH), 70.2 (CH), 71.7 (CH), 76.0 (q), 117.5 (2 × CH), 124.9 (CH), 136.0 (q), 142.4 (2 × q); the signal corresponding to the C2 quaternary carbon atom was impossible to obtain. MS (FAB$^+$) m/z (rel intensity) 603 ($M^+ + 1$, 100). Anal. Calcd for $C_{34}H_{26}Fe_2N_4$: C, 67.80; H, 4.35; N, 9.30. Found: C, 67.65; H, 4.22; N, 9.15.

Acknowledgment. We gratefully acknowledge the financial support from MICINN-Spain, Project CTQ2008-01402, and Fundación Séneca (Agencia de Ciencia y Tecnología de la Región de Murcia), project 04509/GERM/06 (Programa de Ayudas a Grupos de Excelencia de la Región de Murcia, Plan Regional de Ciencia y Tecnología 2007/2010). A.C. also thanks the Ministerio de Educación y Ciencia for a predoctoral grant.

Supporting Information Available: Electrochemical, NMR, UV−vis, and emission spectral data, Job's plots, and detection limit calculations. This material is available free of charge via the Internet at http://pubs.acs.org.